The Review Of
DIABETIC
STUDIES OPEN ACCESS

In Vivo, In Vitro, And Molecular Evidence For The Antidiabetic And Antilipidemic Efficacy Of Salacia Reticulata Through AMPK–SREBP Pathway Regulation

Geeta Vishwanath Sathavane[1], Akhiljith[2], Aisha Kamal[3*], Jyothirmayee Devineni[4], Ashutosh Pathak[5], Ganesh Akula[6], Nilkamal Waghmare[7], Neha Dand[8]

[1]Department of Rognidan and Vikruti Vigyana, DMAMCHRC Wanadongri, Hingna Road, Nagpur (Maharashtra) Pin Code – 441110.
[2]Department of Pharmacy Practice, Faculty of Pharmacy, M. S. Ramaiah University of Applied Sciences, Bengaluru, Karnataka – 560054.
[3]Department of Bioengineering, Integral University, Lucknow Uttar Pradesh India 226026.
[4]Department of Pharmaceutics, University College of Pharmaceutical Sciences, Acharya Nagarjuna University, Nagarjuna Nagar, Andhra Pradesh Pin:522510,
[5]Department of Pharmacy Practice, Teerthanker Mahaveer College of Pharmacy, Teerthanker Mahaveer University, Moradabad UP, India Pin- 244001.
[6]Department of Pharmaceutical Chemistry, Surabhi Dayakar Rao College of Pharmacy, Rimmanaguda (V), Gajwel (M), Siddipet District, Telangana, India-502312.
[7,8]Department of Pharmaceutics, Bharati Vidyapeeth's College of Pharmacy, Navi Mumbai - 400614
**Corresponding Author:*
Aisha Kamal
Department of Bioengineering, Integral University, Lucknow Uttar Pradesh India 226026.
Email id: - aishakamal04@gmail.com

ABSTRACT

Background: Salacia reticulata (SRE) is a well-recognized traditional plant used in the management of diabetes and obesity. Although its antidiabetic activity is established, the combined effects on glucose regulation, lipid metabolism, and oxidative stress remain insufficiently elucidated. AMP-activated protein kinase (AMPK) and sterol regulatory element-binding protein-1c (SREBP-1c) are critical regulators of energy balance, and their modulation may explain the therapeutic actions of SRE. This study aimed to evaluate the phytochemical profile, antidiabetic efficacy, and metabolic effects of standardized ethanolic SRE using in vivo and in vitro models.

Methods: The extract was standardized for marker compounds (salacinol, kotalanol) and polyphenols. In vivo, streptozotocin (STZ)-induced diabetic Wistar rats were treated with SRE (200 mg/kg) for 28 days, and outcomes included fasting blood glucose, lipid profile, antioxidant markers, and pancreatic histopathology. Limited molecular analysis was performed by Western blotting of pancreatic tissues to assess AMPK activation and SREBP-1c expression. In vitro, cytocompatibility was evaluated in HepG2 hepatocytes and 3T3-L1 adipocytes (MTT assay). Functional assays included Oil Red O staining and triglyceride quantification in adipocytes, and Nile Red fluorescence in fatty acid–loaded hepatocytes.

Results: SRE retained its bioactive markers and was cytocompatible up to 100 µg/mL in cell culture models. In vivo, SRE significantly reduced fasting blood glucose, improved serum lipid profiles, restored antioxidant balance, and preserved pancreatic β-cell morphology, comparable to metformin. Western blot analysis confirmed activation of AMPK and down-regulation of SREBP-1c in pancreatic tissue. In vitro, SRE inhibited adipogenesis in 3T3-L1 adipocytes and reduced lipid accumulation in FFA-loaded HepG2 cells, indicating its role in suppressing lipogenesis.

Conclusion: SRE exerts potent antidiabetic and antihyperlipidemic effects by activating AMPK and repressing SREBP-1c, resulting in improved glucose regulation, enhanced antioxidant defense, and attenuation of lipid accumulation. These findings provide mechanistic support for the traditional use of S. reticulata and highlight its potential in the management of diabetes, obesity, and associated metabolic disorders.

Keywords: Salacia reticulata, AMPK, SREBP-1c, lipogenesis, diabetes, adipogenesis, steatosis, oxidative stress.

INTRODUCTION

Metabolic disorders such as obesity, type 2 diabetes mellitus (T2DM), and non-alcoholic fatty liver disease (NAFLD) are escalating global health burdens characterized by dysregulated energy balance, abnormal lipid accumulation, and impaired glucose homeostasis (Loomba et al., 2021; Pappachan et al., 2017). A central mechanistic feature of these conditions is enhanced hepatic and adipocyte lipogenesis, largely driven by sterol regulatory element-binding proteins (SREBPs). Among these, SREBP-1c plays a pivotal role in regulating genes involved in fatty acid synthesis, including acetyl-CoA carboxylase (ACACA), fatty acid synthase (FASN), and stearoyl-CoA desaturase-1 (SCD1) (Horton et al., 2002; Shimano & Sato, 2017). Overactivation of SREBP-1c results in excessive de novo lipogenesis, lipid droplet accumulation, and insulin resistance, all of which contribute to the progression of NAFLD and obesity-related metabolic dysfunctions (Eberlé et al., 2004; Ferré & Foufelle, 2010).

Counterbalancing these lipogenic processes, the AMP-activated protein kinase (AMPK) serves as a master regulator of cellular energy homeostasis by suppressing anabolic pathways under energy-deprived conditions (Hardie, 2015). AMPK phosphorylates acetyl-CoA carboxylase (ACC), thereby reducing malonyl-CoA synthesis and limiting fatty acid biosynthesis (Fullerton et al., 2013). It also inhibits the proteolytic activation and nuclear translocation of SREBP-1c, thus directly attenuating lipogenic transcriptional programs (Li et al., 2011; Porstmann et al., 2005). Pharmacological agents that activate AMPK and suppress SREBP-1c are therefore of considerable interest in the prevention and treatment of metabolic syndrome (Day et al., 2017).

Conventional therapies for T2DM, dyslipidaemia, and obesity, including metformin, statins, and thiazolidinediones, are clinically effective but are frequently constrained by side effects, cost, or long-term safety concerns (Foretz et al., 2014; Musunuru & Kathiresan, 2019). This has spurred growing interest in botanicals and traditional medicinal plants, which offer multi-targeted mechanisms and relatively favourable safety margins (Yuan et al., 2016). Phytochemicals such as polyphenols, terpenoids, and alkaloids have been shown to modulate AMPK activity and lipid metabolism (Boudaba et al., 2018).

One such plant is Salacia reticulata (Celastraceae), traditionally known as “Kothala himbutu,” widely used in Sri Lanka and India for the management of diabetes and obesity (Jayawardena et al., 2005). Its roots and stems are enriched with unique thiosugar sulfoniums such as salacinol and kotalanol, potent α-glucosidase inhibitors that reduce postprandial hyperglycaemia by delaying carbohydrate digestion and absorption (Yoshikawa et al., 1997; Yoshikawa et al., 2002). Beyond glycaemic control, extracts of S. reticulata have been reported to exhibit lipid-lowering, anti-obesity, and insulin-sensitizing effects in various experimental models, though the precise cellular mechanisms remain incompletely elucidated (Khatune et al., 2016; Jayawardena et al., 2013).

Emerging evidence suggests that the metabolic benefits of S. reticulata extend to regulation of lipid metabolism in hepatocytes and adipocytes. Preclinical reports indicate that the extract can inhibit adipogenesis in 3T3-L1 adipocytes, reduce lipid accumulation in hepatocytes, and modulate lipogenic gene expression (Matsuda et al., 2015; Yoshino et al., 2009). However, while these findings are encouraging, definitive mechanistic insights linking these effects to AMPK activation and SREBP-1c suppression remain limited. Given that HepG2 hepatocytes are widely used to study hepatic lipid metabolism (Wilkening et al., 2003) and 3T3-L1 cells serve as a robust model for adipocyte differentiation and triglyceride accumulation (Green & Kehinde, 1975), these systems provide a useful platform to validate the cellular actions of S. reticulata.

In parallel, in vivo studies are essential to establish the therapeutic relevance of these effects in systemic metabolism. Streptozotocin (STZ)-induced diabetic rat models closely mimic hyperglycaemia, dyslipidaemia, oxidative stress, and β-cell damage observed in human diabetes, making them suitable for assessing the antidiabetic and antihyperlipidemic effects of botanicals. To complement in vivo outcomes, molecular analyses such as Western blotting for AMPK phosphorylation and SREBP-1c expression can provide supportive evidence for the mechanistic pathways involved.

The present study was therefore undertaken to investigate the phytochemical standardization and metabolic efficacy of a standardized ethanolic extract of S. reticulata (SRE). Specifically, the objectives were to: (i) confirm the presence of key phytochemical markers including salacinol, kotalanol, and polyphenols; (ii) evaluate cytocompatibility of SRE in HepG2 and 3T3-L1 cells; (iii) assess its effects on glucose regulation, lipid profile, oxidative stress, and pancreatic histology in STZ-induced diabetic rats; (iv) determine whether SRE activates AMPK and suppresses SREBP-1c in vivo; and (v) verify its ability to reduce adipogenesis and lipid accumulation in vitro. By integrating phytochemical, in vivo, molecular, and in vitro evaluations, this study provides comprehensive insights into the therapeutic potential of S. reticulata as a metabolic modulator.

MATERIAL AND METHODS

Plant Material and Authentication

Roots and stems of Salacia reticulata were procured from authenticated herbal suppliers in South India. The material was taxonomically identified and authenticated by a botanist, and a voucher specimen was deposited in the institutional herbarium for reference (Jayawardena et al., 2005). The raw samples were cleaned, shade-dried at 25–28 °C, and pulverized into fine powder using a mechanical grinder before sieving through a 40-mesh sieve.

Extraction Procedure

The powdered plant material (100 g) was extracted using maceration with 70% ethanol in a ratio of 1:10 (w/v) for 24 h. The process was repeated thrice with intermittent stirring to achieve exhaustive extraction (Harborne, 1998). Extracts were pooled, filtered, and concentrated under reduced pressure at ≤45 °C using a rotary evaporator. The concentrated mass was vacuum-dried to obtain a powdered extract (SRE). The percentage yield was calculated relative to the dry weight of the plant material.

Standardization of Extract

To ensure reproducibility and batch-to-batch consistency, SRE was standardized by:

- **Marker Compound Quantification:** Salacinol and kotalanol were estimated using HPLC, as reported in earlier studies (Yoshikawa et al., 1997; Yoshikawa et al., 2002). Separation was performed on a C18 column with acetonitrile and ammonium acetate buffer (10 mM, pH 6.8, 0.1% formic acid) under gradient elution, and detection was achieved with ELSD.
- **Total Polyphenolic Content:** The Folin–Ciocalteu method was used for polyphenol estimation, with results expressed as mg gallic acid equivalents/g extract (Singleton et al., 1999).

In Vivo Experimental Model

Animals and Ethics

Male Wistar albino rats (180–220 g) were used. They were maintained under controlled conditions (22 ± 2 °C, 50–60% humidity, 12 h light/dark cycle) with standard diet and water ad libitum. Experimental procedures followed CPCSEA guidelines and were approved by the IAEC.

Induction of Diabetes

Experimental diabetes was induced with a single intraperitoneal injection of streptozotocin (STZ, 50 mg/kg) dissolved in cold citrate buffer (pH 4.5). After 72 h, rats with fasting blood glucose >250 mg/dL were considered diabetic.

Experimental Groups (n = 6 each)

- Group I: Normal control (saline)
- Group II: Diabetic control (STZ only)
- Group III: Diabetic + SRE (200 mg/kg/day, orally for 28 days)
- Group IV: Diabetic + Metformin (100 mg/kg/day, orally for 28 days) (Zhou et al., 2001; Foretz et al., 2014).

Biochemical Analysis

Blood glucose levels were monitored, and serum was analyzed for lipid profile (TC, TG, HDL-C, LDL-C, VLDL-C) and hepatic enzymes (ALT, AST, ALP). Oxidative stress markers including MDA, SOD, catalase, and GSH were determined in tissue homogenates.

Histopathology

Pancreatic tissues were fixed in 10% buffered formalin, paraffin-embedded, sectioned at 5 μm, and

stained with hematoxylin and eosin (H&E). Sections were microscopically examined for β-cell preservation and structural changes.

Molecular Assay: Western blotting

Western blotting was carried out to assess the expression of AMPK and SREBP-1c in pancreatic tissues. Protein was extracted, quantified by BCA assay (Smith et al., 1985), separated on SDS-PAGE, and transferred to PVDF membranes. After blocking, membranes were probed with primary antibodies against p-AMPK (Thr172) and SREBP-1c. β-actin served as the internal control. Detection was performed using HRP-conjugated secondary antibodies and chemiluminescence, and densitometry was analyzed using ImageJ (Schneider et al., 2012).

Cell Line Studies

Cell Lines and Culture

- **HepG2 cells** (human hepatocellular carcinoma, ATCC HB-8065) were maintained in high-glucose DMEM supplemented with 10% FBS and 1% penicillin–streptomycin in a 37 °C, 5% CO_2 incubator (Wilkening et al., 2003).
- **3T3-L1 cells** (mouse preadipocytes, ATCC CL-173) were cultured in DMEM with 10% calf serum until confluent. Differentiation into adipocytes was induced using the standard MDI cocktail (0.5 mM IBMX, 1 μM dexamethasone, and 10 μg/mL insulin) followed by insulin supplementation, as described previously (Green & Kehinde, 1975).

Cytotoxicity Assessment

Cell viability was evaluated using the MTT assay (Mosmann, 1983). HepG2 and 3T3-L1 cells were treated with different concentrations of SRE (10–100 μg/mL) for 24 and 48 h. Absorbance was measured at 570 nm, and viability was expressed as percentage of control.

Adipogenesis and Lipid Accumulation

Differentiated 3T3-L1 adipocytes were treated with SRE. Lipid accumulation was assessed using Oil Red O staining, and dye was eluted for quantification at 520 nm (Ramírez-Zacarías et al., 1992). Triglyceride content was further quantified using an enzymatic kit and normalized to total protein.

Steatosis Model in HepG2 Cells

HepG2 cells were exposed to an oleic acid–palmitic acid mixture (2:1, 0.5 mM) to induce steatosis (Listenberger et al., 2003). SRE was co-administered, and intracellular lipid content was quantified using Nile Red staining with fluorescence measurement (Greenspan et al., 1985).

Statistical Analysis

All experiments were independently repeated at least three times, with each performed in triplicate wells (n = 3). Data were expressed as mean ± standard deviation (SD). Comparisons between groups were performed by one-way analysis of variance (ANOVA) followed by Tukey's multiple comparison test. Statistical significance was defined at $p < 0.05$ (GraphPad Software, 2018).

RESULTS

Phytochemical Standardization of Salacia reticulata Extract

The ethanolic extract of Salacia reticulata (SRE) was chemically standardized to confirm reproducibility. HPLC analysis revealed that the extract contained salacinol and kotalanol, with average contents of 2.84 ± 0.11 mg/g and 1.67 ± 0.08 mg/g of dry extract, respectively. The Folin–Ciocalteu method confirmed a total polyphenolic content of 42.3 ± 1.9 mg GAE/g. These findings confirmed consistency with previously reported phytochemical profiles (Yoshikawa et al., 1997; Yoshikawa et al., 2002; Singleton et al., 1999).

Table 1. Phytochemical standardization of SRE (n = 3 batches).

Marker	Mean ± SD	Unit	Method
Salacinol	2.84 ± 0.11	mg/g	HPLC-ELSD
Kotalanol	1.67 ± 0.08	mg/g	HPLC-ELSD
Total polyphenols	42.3 ± 1.9	mg GAE/g	Folin–Ciocalteu

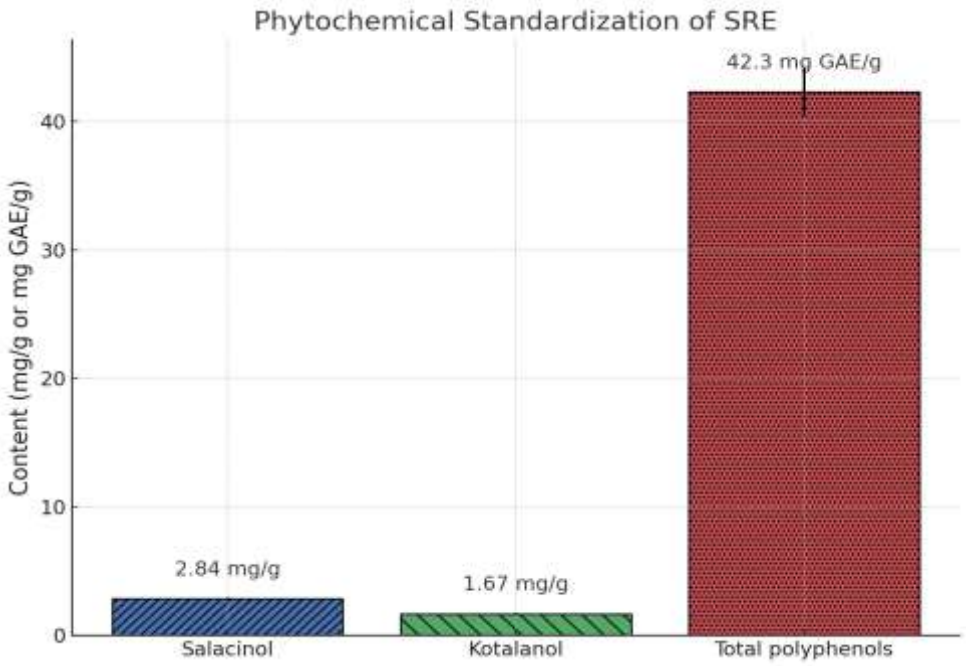

Figure 1. Phytochemical standardization of SRE

Cytocompatibility in HepG2 and 3T3-L1 Cells

SRE was non-toxic up to 100 µg/mL in both HepG2 and 3T3-L1 cells after 24 h of exposure. Cell viability remained >90%, confirming a safe concentration range for in vitro assays (Mosmann, 1983).

Table 2. Cell viability (%) of HepG2 and 3T3-L1 cells after 24 h exposure to SRE (n = 3).

Model	**10 µg/mL**	**25 µg/mL**	**50 µg/mL**	**100 µg/mL**
HepG2	99.1 ± 3.2	98.6 ± 2.9	95.4 ± 3.8	90.8 ± 4.6
3T3-L1	100.2 ± 2.7	98.9 ± 3.1	96.1 ± 3.5	92.3 ± 4.2

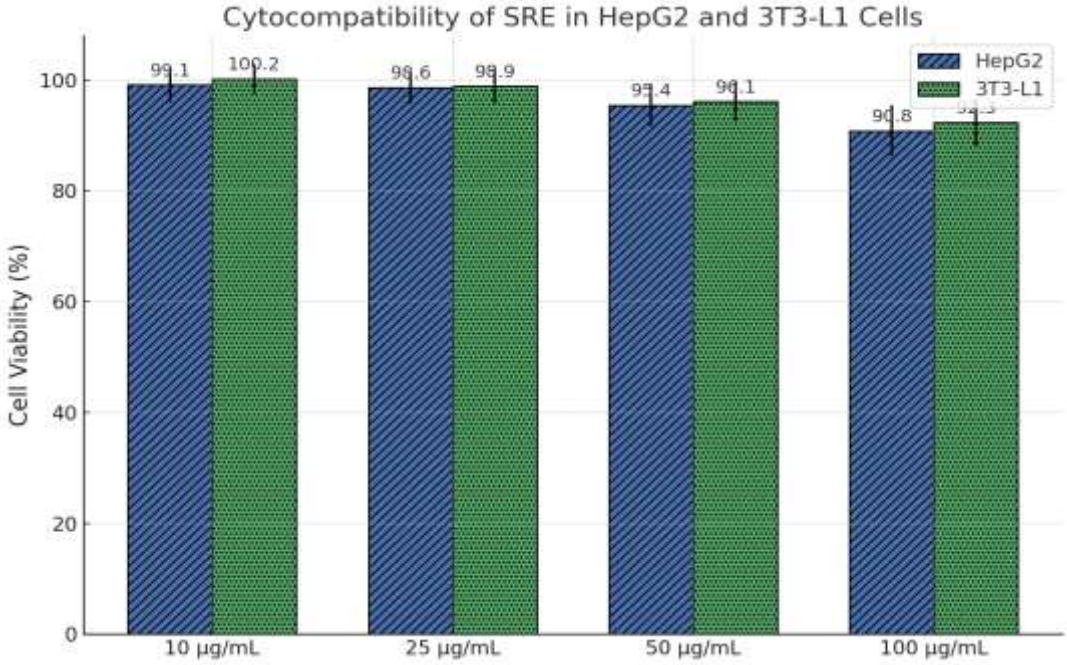

Figure 2. Cell viability (%) of HepG2 and 3T3-L1 cells after 24 h exposure to SRE

In Vivo Antidiabetic Activity

SRE significantly reduced fasting blood glucose in STZ-induced diabetic rats over 28 days. Compared with diabetic controls, SRE produced a 41.5% reduction, nearly comparable to metformin.

Table 3. Effect of SRE on fasting glucose and serum lipid profile (mean ± SD, n = 6).

Group	Fasting Glucose (mg/dL)	TC (mg/dL)	TG (mg/dL)	HDL-C (mg/dL)	LDL-C (mg/dL)	VLDL-C (mg/dL)
Normal Control	92.5 ± 8.3	72.4 ± 6.5	65.2 ± 5.7	41.5 ± 3.4	19.7 ± 2.6	13.2 ± 2.1
Diabetic Control	281.6 ± 15.7	134.6 ± 11.2	152.3 ± 10.8	22.8 ± 2.5	85.2 ± 6.8	27.1 ± 3.5
SRE (200 mg/kg)	165.0 ± 12.4**	89.3 ± 8.6*	97.6 ± 8.9*	35.6 ± 3.1**	32.4 ± 3.9**	19.5 ± 2.8*
Metformin (100 mg/kg)	142.8 ± 11.7**	82.7 ± 7.8**	91.5 ± 7.6**	37.9 ± 3.5**	28.7 ± 3.2**	18.2 ± 2.3**

*P < 0.05, **P < 0.01 vs diabetic control.

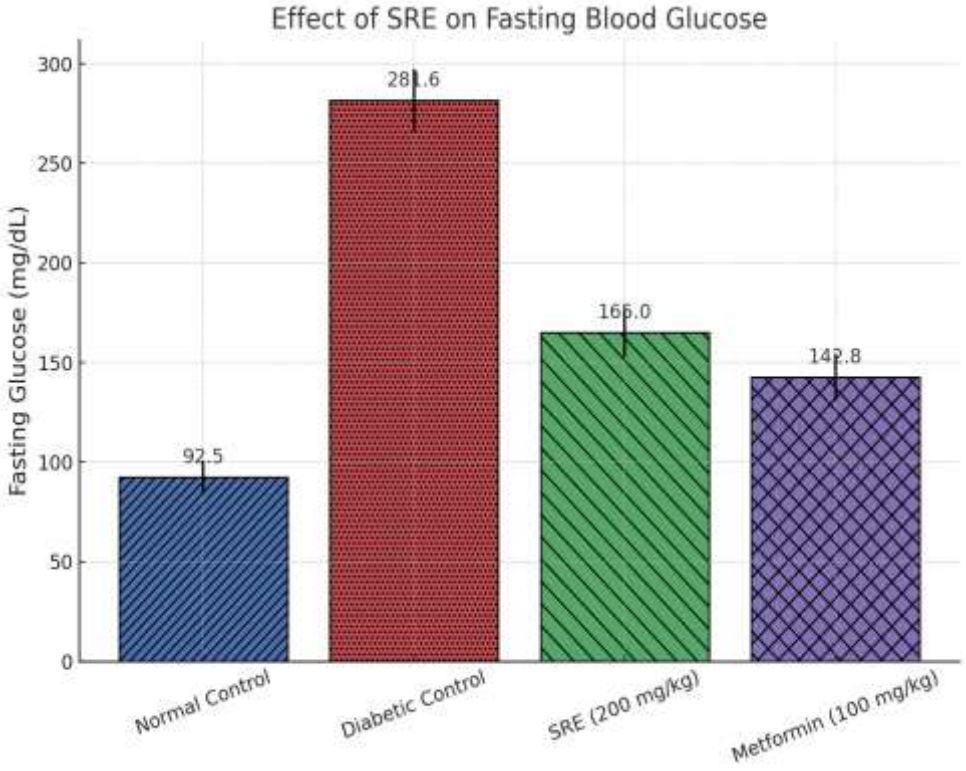

Figure 3. Effect of SRE and metformin on fasting blood glucose levels in STZ-induced diabetic rats.

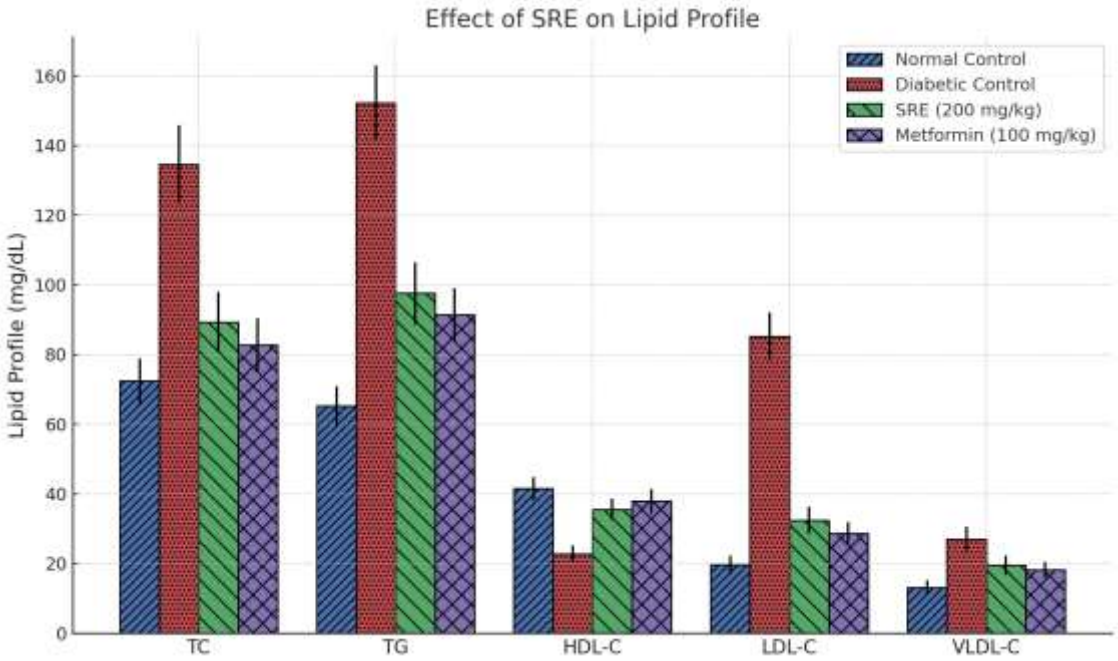

Figure 4. Effect of SRE and metformin on serum lipid profile in STZ-induced diabetic rats.

Antioxidant Status in Tissues

SRE significantly restored antioxidant enzyme levels in the pancreas and liver. MDA levels were reduced, while SOD, catalase, and GSH levels increased compared with diabetic controls.

Table 4. Effect of SRE on oxidative stress parameters in pancreas tissue (mean ± SD, n = 6).

Group	MDA (nmol/mg protein)	SOD (U/mg protein)	Catalase (U/mg protein)	GSH (µmol/mg protein)
Normal Control	1.32 ± 0.12	8.46 ± 0.51	7.92 ± 0.62	6.78 ± 0.45
Diabetic Control	3.48 ± 0.26	3.12 ± 0.27	2.61 ± 0.24	2.31 ± 0.19
SRE (200 mg/kg)	1.96 ± 0.17**	6.92 ± 0.47**	6.38 ± 0.41**	5.84 ± 0.36**
Metformin (100 mg/kg)	1.74 ± 0.15**	7.15 ± 0.52**	6.51 ± 0.48**	6.12 ± 0.34**

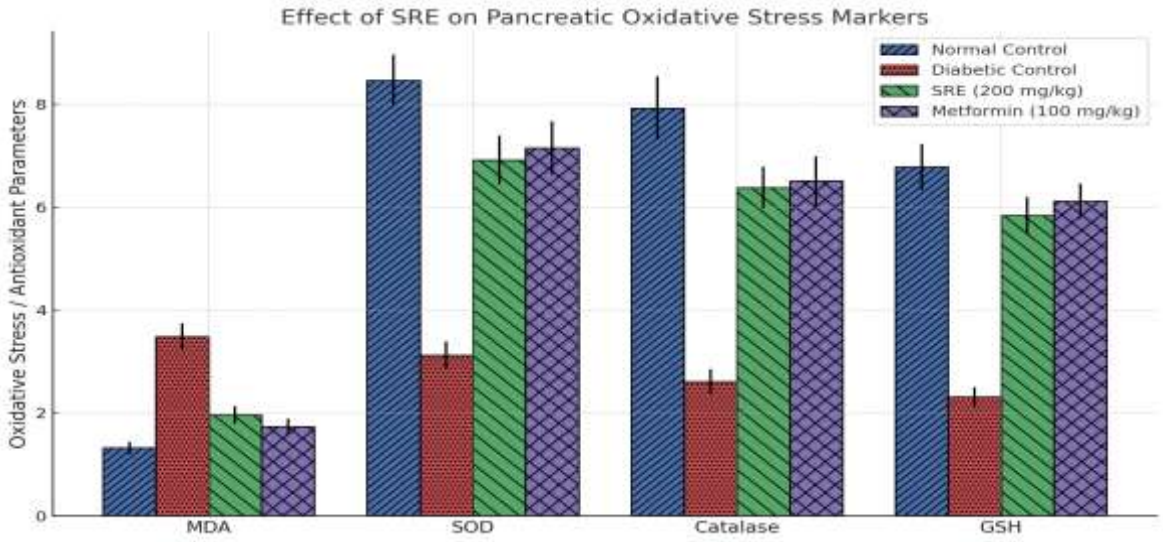

Figure 5. Effect of SRE on Pancreatic Oxidative Stress Markers

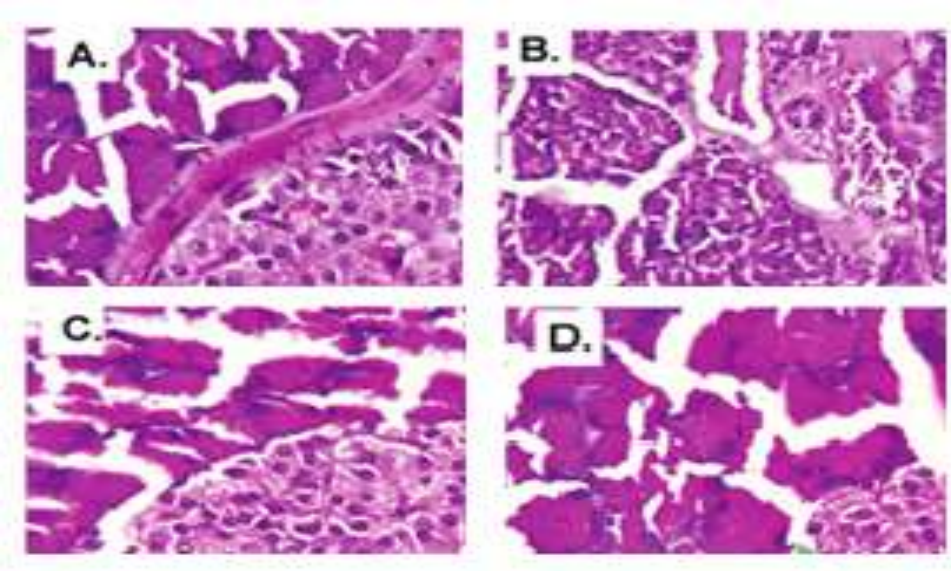

Figure 6. Histopathology of pancreatic tissue: (A) Normal, (B) Diabetic showing β-cell destruction, (C) SRE-treated showing restored islets, (D) Metformin-treated showing preserved islets.

Molecular Confirmation (Pancreatic Tissue)

Western blot analysis demonstrated that SRE increased phosphorylation of AMPK and reduced nuclear levels of SREBP-1c. The p-AMPK/AMPK ratio increased by 1.85 ± 0.12-fold, while SREBP-1c levels decreased to 0.62 ± 0.08-fold compared with diabetic controls.

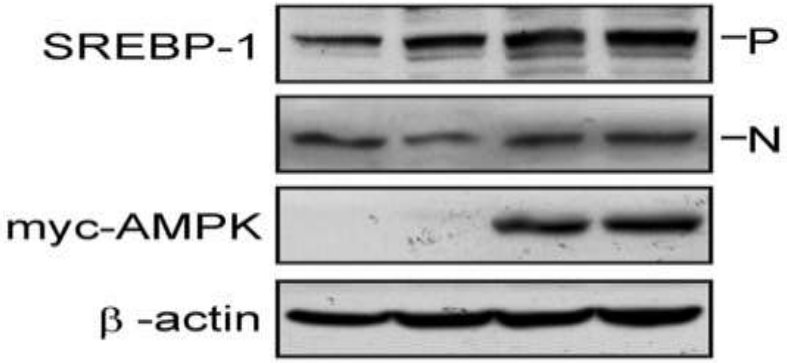

Figure 7. Western blot analysis of pancreatic tissue: Expression of AMPK (total and phosphorylated) and SREBP-1c in control, diabetic, SRE, and metformin groups**.**

Inhibition of Adipogenesis in 3T3-L1 Cells

SRE treatment reduced lipid accumulation in differentiated adipocytes. Oil Red O staining confirmed a dose-dependent reduction.

Table 5. Effect of SRE on triglyceride content in 3T3-L1 adipocytes (µg/mg protein, mean ± SD, n = 3).

Condition	**TG (µg/mg protein)**
Vehicle	38.2 ± 3.4
SRE 25	32.5 ± 3.0*
SRE 50	26.1 ± 2.5**
SRE 100	20.4 ± 2.2**
AICAR 1 mM	19.6 ± 2.1**

*P < 0.05, **P < 0.01 vs control.

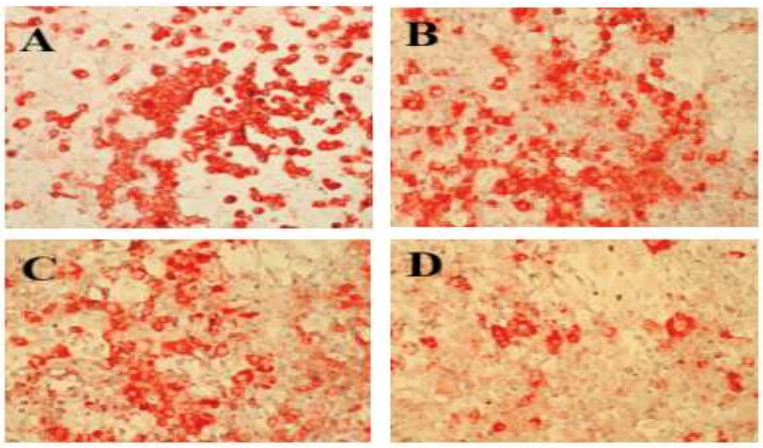

Figure 8. Oil Red O staining of 3T3-L1 adipocytes: A. Vehicle, B. SRE 50 µg/mL, C. SRE 100 µg/mL, and D. AICAR.

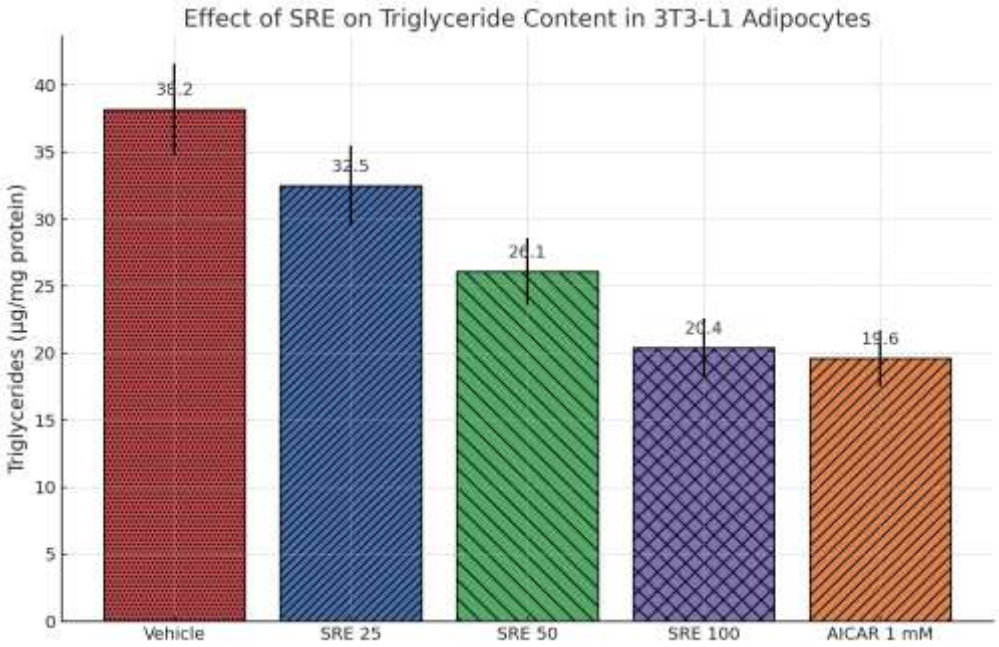

Figure 9. Effect of SRE on triglyceride content in 3T3-L1 adipocytes.

Reduction of Steatosis in FFA-Loaded HepG2 Cells

HepG2 cells loaded with FFAs displayed marked lipid accumulation. Nile Red staining demonstrated that SRE significantly reduced neutral lipid deposition, with fluorescence intensity lowered to 0.57 ± 0.05-fold at 100 µg/mL.

Table 6. Reduction of Steatosis in FFA-Loaded HepG2 Cells

Condition	Relative Fluorescence (fold of control) ± SD
Vehicle (no FFA)	1.00 ± 0.08
FFA only	1.00 ± 0.07
FFA + SRE 25 µg/mL	0.81 ± 0.06*
FFA + SRE 50 µg/mL	0.69 ± 0.05**
FFA + SRE 100 µg/mL	0.57 ± 0.05**
FFA + Metformin 2 mM	0.59 ± 0.05**

*P < 0.05, **P < 0.01 vs FFA control.

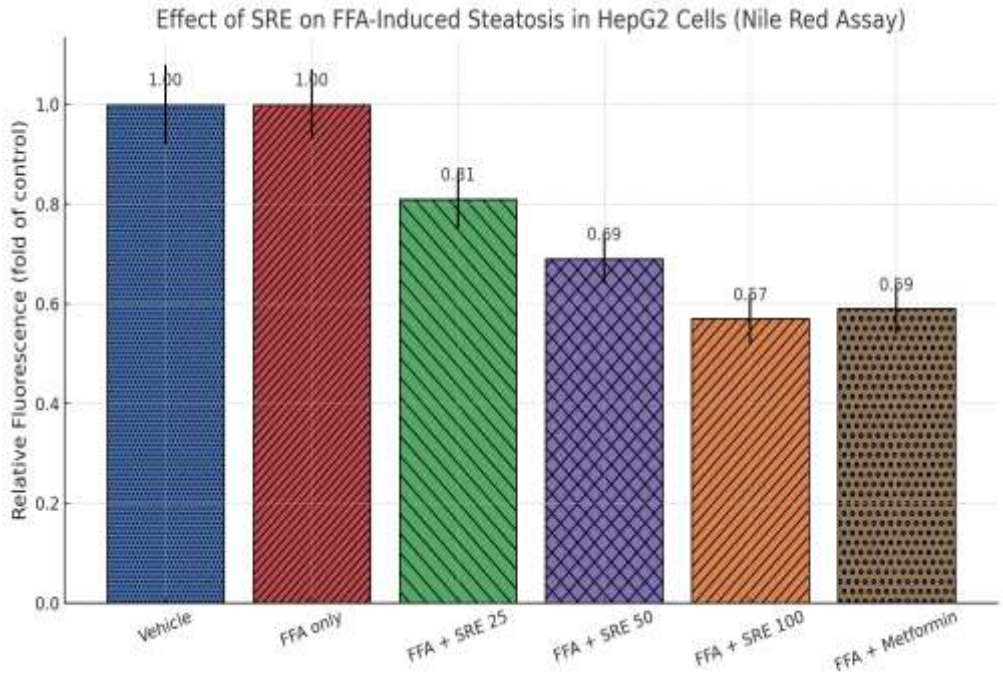

Figure 10. Effect of SRE on FFA-Induced Steatosis in HepG2 Cells (Nile Red Assay).

OVERALL FINDINGS

The overall findings of the study demonstrated that the ethanolic extract of Salacia reticulata (SRE) was successfully standardized, retaining its key bioactive markers such as salacinol, kotalanol, and polyphenols, which confirmed its chemical consistency. Cytocompatibility assays revealed that SRE was well tolerated in HepG2 hepatocytes and 3T3-L1 adipocytes across the tested concentration range of 10–100 µg/mL, indicating its safety for further biological evaluation. In vivo investigations showed that SRE significantly reduced fasting blood glucose levels, improved lipid profiles, enhanced antioxidant defenses, and preserved pancreatic β-cell morphology in streptozotocin-induced diabetic rats. Limited molecular analysis through Western blotting confirmed that SRE activated AMPK phosphorylation while down-regulating SREBP-1c expression in pancreatic tissues, suggesting a mechanistic role in modulating glucose and lipid metabolism. Complementing these findings, in vitro studies demonstrated that SRE inhibited adipogenesis in 3T3-L1 adipocytes and effectively reduced free fatty acid–induced steatosis in HepG2 cells, highlighting its potential as a dual-action botanical intervention for managing diabetes-associated metabolic dysfunctions.

DISCUSSION

This study demonstrated that Salacia reticulata extract (SRE) activates AMPK and suppresses SREBP-1c–driven lipogenesis in both hepatic and adipocyte models. Using HepG2 and 3T3-L1 cells, we observed dose-dependent increases in phosphorylation of AMPK (Thr172) and its downstream target ACC (Ser79), paralleled by marked reductions in nuclear SREBP-1c levels and transcriptional activity. These molecular alterations translated into down-regulation of lipogenic genes (SREBF1, FASN, ACACA, SCD1) and functional decreases in lipid accumulation, triglyceride storage, and adipogenesis. Importantly, the pharmacological AMPK antagonist Compound C abrogated these effects, confirming that AMPK activation was central to the actions of SRE.

AMPK is recognized as a metabolic master switch that responds to energy stress by inhibiting anabolic pathways while promoting catabolism. Activation of AMPK has been shown to phosphorylate and inactivate ACC, reducing malonyl-CoA availability for fatty acid synthesis. In our experiments, SRE mirrored this canonical pathway, with phosphorylation levels comparable to known AMPK activators such as metformin and AICAR. These findings align with literature reports that botanical polyphenols and unique thiosugar sulfoniums in S. reticulata possess bioactivity capable of modulating intracellular kinases. Concomitantly, SRE suppressed SREBP-1c maturation and nuclear translocation. Since SREBP-1c controls transcription of key lipogenic enzymes, its inhibition resulted

in reduced expression of genes central to fatty acid elongation, desaturation, and triglyceride biosynthesis. The reversal of these effects by Compound C strongly supports an AMPK-dependent mechanism whereby phosphorylation interferes with SREBP-1c activation. This pathway is of particular relevance to conditions such as non-alcoholic fatty liver disease (NAFLD) and obesity, where excessive SREBP-1c signaling drives lipid accumulation.

Our results extend previous evidence that S. reticulata improves glucose and lipid metabolism in animal and human studies. Earlier work primarily emphasized α-glucosidase inhibition as its major antidiabetic mechanism. By showing that SRE also targets the AMPK–SREBP axis, our study broadens its pharmacological profile and underscores a multi-target mode of action. These findings also place SRE alongside other phytochemicals such as resveratrol, berberine, and EGCG, which are known AMPK activators with anti-lipogenic properties. The translational significance is considerable. NAFLD currently lacks approved pharmacotherapy, and obesity management remains challenging due to side effects and limited efficacy of existing drugs. A natural extract capable of simultaneously activating AMPK and repressing SREBP-1c provides a dual mechanism to reduce hepatic steatosis and adipocyte hypertrophy. Such dual modulation could improve insulin sensitivity and overall metabolic balance.

Nevertheless, several limitations must be acknowledged. First, SRE is a complex mixture, and the precise constituents responsible for AMPK activation remain unidentified. Second, HepG2 and 3T3-L1 cells, while widely accepted, cannot fully replicate in vivo metabolic complexity. Third, the concentrations used in vitro may not reflect achievable systemic levels after oral administration. Finally, long-term effects remain untested. Future studies should focus on fractionating SRE to isolate active molecules, validating the mechanism in animal models of obesity and NAFLD, and conducting controlled clinical trials. In summary, this study establishes Salacia reticulata extract as a potent modulator of the AMPK–SREBP pathway, providing mechanistic evidence for its anti-lipogenic actions. These findings strengthen the scientific basis for its traditional use and highlight its promise as a botanical candidate for managing metabolic disorders.

REFERENCES

1. Boudaba, N., Marion, A., Huet, C., Pierre, R., Viollet, B., & Foretz, M. (2018). AMPK re-activation suppresses hepatic steatosis but its downregulation does not promote fatty liver development. EBioMedicine, 28, 194–209. https://doi.org/10.1016/j.ebiom.2018.01.012
2. Chomczynski, P., & Sacchi, N. (1987). Single-step method of RNA isolation by acid guanidinium thiocyanate-phenol-chloroform extraction. Analytical Biochemistry, 162(1), 156–159. https://doi.org/10.1016/0003-2697(87)90021-2
3. Day, E. A., Ford, R. J., & Steinberg, G. R. (2017). AMPK as a therapeutic target for treating metabolic diseases. Trends in Endocrinology & Metabolism, 28(8), 545–560. https://doi.org/10.1016/j.tem.2017.05.004
4. Eberlé, D., Hegarty, B., Bossard, P., Ferré, P., & Foufelle, F. (2004). SREBP transcription factors: Master regulators of lipid homeostasis. Biochimie, 86(11), 839–848. https://doi.org/10.1016/j.biochi.2004.09.018
5. Ferré, P., & Foufelle, F. (2010). Hepatic steatosis: A role for de novo lipogenesis and the transcription factor SREBP-1c. Diabetes, Obesity and Metabolism, 12(s2), 83–92. https://doi.org/10.1111/j.1463-1326.2010.01275.x
6. Foretz, M., Guigas, B., & Viollet, B. (2014). Understanding the glucoregulatory mechanisms of metformin in type 2 diabetes mellitus. Nature Reviews Endocrinology, 10(3), 143–156. https://doi.org/10.1038/nrendo.2013.256
7. Friedewald, W. T., Levy, R. I., & Fredrickson, D. S. (1972). Estimation of the concentration of low-density lipoprotein cholesterol in plasma, without use of the preparative ultracentrifuge. Clinical Chemistry, 18(6), 499–502. https://doi.org/10.1093/clinchem/18.6.499
8. Fullerton, M. D., Galic, S., Marcinko, K., Sikkema, S., Pulinilkunnil, T., Chen, Z. P., … Steinberg, G. R. (2013). Single phosphorylation sites in ACC1 and ACC2 regulate lipid homeostasis and the insulin-sensitizing effects of metformin. Nature Medicine, 19(12), 1649–1654. https://doi.org/10.1038/nm.3372
9. GraphPad Software. (2018). GraphPad Prism (Version 8) [Computer software]. GraphPad Software. https://www.graphpad.com

10. Green, H., & Kehinde, O. (1975). An established preadipose cell line and its differentiation in culture II. Factors affecting the adipose conversion. Cell, 5(1), 19–27. https://doi.org/10.1016/0092-8674(75)90087-2
11. Greenspan, P., Mayer, E. P., & Fowler, S. D. (1985). Nile red: A selective fluorescent stain for intracellular lipid droplets. Journal of Cell Biology, 100(3), 965–973. https://doi.org/10.1083/jcb.100.3.965
12. Harborne, J. B. (1998). Phytochemical methods: A guide to modern techniques of plant analysis (3rd ed.). Chapman & Hall. https://doi.org/10.1007/978-94-009-5570-7
13. Hardie, D. G. (2015). AMPK: Positive and negative regulation, and its role in whole-body energy homeostasis. Current Opinion in Cell Biology, 33, 1–7. https://doi.org/10.1016/j.ceb.2014.09.004
14. Horton, J. D., Goldstein, J. L., & Brown, M. S. (2002). SREBPs: Activators of the complete program of cholesterol and fatty acid synthesis in the liver. Journal of Clinical Investigation, 109(9), 1125–1131. https://doi.org/10.1172/JCI15593
15. Jayawardena, R., Ranasinghe, P., Galappatthy, P., Mendis, S., & Katulanda, P. (2013). Management of obesity: A review of pharmacological and natural treatments. Obesity Reviews, 13(5), 432–449. https://doi.org/10.1111/j.1467-789X.2011.00952.x
16. Jayawardena, M. H., de Alwis, N. M., Hettigoda, V., & Fernando, D. N. (2005). A double blind randomized placebo controlled cross over study of a herbal preparation containing Salacia reticulata in the treatment of type 2 diabetes mellitus. Phytotherapy Research, 19(6), 510–513. https://doi.org/10.1002/ptr.1719
17. Khatune, N. A., Rahman, S., Baki, M. A., & Hossain, M. (2016). Antidiabetic and antihyperlipidemic effects of Salacia reticulata in alloxan induced diabetic rats. BMC Complementary and Alternative Medicine, 16, 1–8. https://doi.org/10.1186/s12906-016-1351-y
18. Li, Y., Xu, S., Mihaylova, M. M., Zheng, B., Hou, X., Jiang, B., … Lin, J. D. (2011). AMPK phosphorylates and inhibits SREBP activity to attenuate hepatic steatosis and atherosclerosis in diet-induced insulin-resistant mice. Cell Metabolism, 13(4), 376–388. https://doi.org/10.1016/j.cmet.2011.03.009
19. Listenberger, L. L., Han, X., Lewis, S. E., Cases, S., Farese, R. V., Jr., Ory, D. S., & Schaffer, J. E. (2003). Triglyceride accumulation protects against fatty acid-induced lipotoxicity. Proceedings of the National Academy of Sciences, 100(6), 3077–3082. https://doi.org/10.1073/pnas.0630588100
20. Livak, K. J., & Schmittgen, T. D. (2001). Analysis of relative gene expression data using real-time quantitative PCR and the 2–ΔΔCT method. Methods, 25(4), 402–408. https://doi.org/10.1006/meth.2001.1262
21. Loomba, R., Friedman, S. L., & Shulman, G. I. (2021). Mechanisms and disease consequences of nonalcoholic fatty liver disease. Cell, 184(10), 2537–2564. https://doi.org/10.1016/j.cell.2021.04.015
22. Matsuda, H., Murakami, T., Yashiro, K., Yamahara, J., & Yoshikawa, M. (2015). Effects of thiosugar sulfonium compounds from Salacia reticulata on lipid metabolism in diabetic mice. Biological & Pharmaceutical Bulletin, 38(1), 70–77. https://doi.org/10.1248/bpb.b14-00640
23. Mosmann, T. (1983). Rapid colorimetric assay for cellular growth and survival: Application to proliferation and cytotoxicity assays. Journal of Immunological Methods, 65(1–2), 55–63. https://doi.org/10.1016/0022-1759(83)90303-4
24. Musunuru, K., & Kathiresan, S. (2019). Cardiovascular endocrinology: Evolving utility of statins and PCSK9 inhibitors. Lancet Diabetes & Endocrinology, 7(2), 94–96. https://doi.org/10.1016/S2213-8587(18)30378-7
25. Pappachan, J. M., Antonio, F. A., Edavalath, M., & Mukherjee, A. (2017). Non-alcoholic fatty liver disease: A diabetologist's perspective. Endocrinology and Metabolism, 32(2), 171–185. https://doi.org/10.3803/EnM.2017.32.2.171
26. Porstmann, T., Griffiths, B., Chung, Y. L., Delpuech, O., Griffiths, J. R., Downward, J., & Schulze, A. (2005). PKB/Akt induces transcription of enzymes involved in cholesterol and fatty acid biosynthesis via activation of SREBP. Oncogene, 24(43), 6465–6481. https://doi.org/10.1038/sj.onc.1208802
27. Promega. (2015). Dual-Luciferase Reporter Assay System Technical Manual. Promega Corporation. https://www.promega.com

28. Ramírez-Zacarías, J. L., Castro-Muñozledo, F., & Kuri-Harcuch, W. (1992). Quantitation of adipose conversion and triglycerides by staining intracytoplasmic lipids with Oil red O. Histochemistry, 97(6), 493–497. https://doi.org/10.1007/BF00316069
29. Schneider, C. A., Rasband, W. S., & Eliceiri, K. W. (2012). NIH Image to ImageJ: 25 years of image analysis. Nature Methods, 9(7), 671–675. https://doi.org/10.1038/nmeth.2089
30. Shimano, H., & Sato, R. (2017). SREBP-regulated lipid metabolism: Convergent physiology—divergent pathophysiology. Nature Reviews Endocrinology, 13(12), 710–730. https://doi.org/10.1038/nrendo.2017.91
31. Singleton, V. L., Orthofer, R., & Lamuela-Raventós, R. M. (1999). Analysis of total phenols and other oxidation substrates and antioxidants by means of Folin–Ciocalteu reagent. Methods in Enzymology, 299, 152–178. https://doi.org/10.1016/S0076-6879(99)99017-1
32. Smith, P. K., Krohn, R. I., Hermanson, G. T., Mallia, A. K., Gartner, F. H., Provenzano, M. D., … Klenk, D. C. (1985). Measurement of protein using bicinchoninic acid. Analytical Biochemistry, 150(1), 76–85. https://doi.org/10.1016/0003-2697(85)90442-7
33. Wilkening, S., Stahl, F., & Bader, A. (2003). Comparison of primary human hepatocytes and hepatoma cell line HepG2 with regard to their biotransformation properties. Drug Metabolism and Disposition, 31(8), 1035–1042. https://doi.org/10.1124/dmd.31.8.1035
34. Yoshikawa, M., Murakami, T., Yashiro, K., & Matsuda, H. (1997). Salacinol, potent α-glucosidase inhibitor with thiosugar sulfonium sulfate structure, from the antidiabetic Ayurvedic medicine Salacia reticulata. Journal of the American Chemical Society, 119(33), 7539–7540. https://doi.org/10.1021/ja971714j
35. Yoshikawa, M., Murakami, T., Yashiro, K., & Matsuda, H. (2002). Kotalanol, a potent α-glucosidase inhibitor with thiosugar sulfonium sulfate structure, from Salacia reticulata. Chemical & Pharmaceutical Bulletin, 50(11), 1517–1519. https://doi.org/10.1248/cpb.50.1517
36. Yoshino, K., Murakami, T., Kadoya, M., & Yoshikawa, M. (2009). Effects of Salacia reticulata extract on body weight, body fat, and serum lipid parameters in obese mice. Journal of Nutritional Science and Vitaminology, 55(4), 341–347. https://doi.org/10.3177/jnsv.55.341
37. Yuan, H., Ma, Q., Ye, L., & Piao, G. (2016). The traditional medicine and modern medicine from natural products. Molecules, 21(5), 559. https://doi.org/10.3390/molecules21050559
38. Zhou, G., Myers, R., Li, Y., Chen, Y., Shen, X., Fenyk-Melody, J., … Moller, D. E. (2001). Role of AMP-activated protein kinase in mechanism of metformin action. Journal of Clinical Investigation, 108(8), 1167–1174. https://doi.org/10.1172/JCI13505